IOPscience iopscience.iop.org

Home Search Collections Journals About Contact us My IOPscience

Nonlinear algorithm for the solution of the Kohn–Sham equations in solids

This article has been downloaded from IOPscience. Please scroll down to see the full text article.

2005 J. Phys.: Condens. Matter 17 3701

(http://iopscience.iop.org/0953-8984/17/25/001)

View the table of contents for this issue, or go to the journal homepage for more

Download details:
IP Address: 129.252.86.83
The article was downloaded on 28/05/2010 at 05:04

Please note that terms and conditions apply.

INSTITUTE OF PHYSICS PUBLISHING JOURNAL OF PHYSICS: CONDENSED MATTER

J. Phys.: Condens. Matter **17** (2005) 3701–3715 doi:10.1088/0953-8984/17/25/001

Nonlinear algorithm for the solution of the Kohn–Sham equations in solids

Jian Wang[1], Yu Wang[1], Shaoying Yu[1] and Dietmar Kolb[2]

[1] School of Science, Huzhou University, Zhejiang 313000, People's Republic of China
[2] Department of Physics, University of Kassel, Germany

Received 10 November 2004, in final form 18 May 2005
Published 10 June 2005
Online at stacks.iop.org/JPhysCM/17/3701

Abstract

We apply a nonlinear multigrid algorithm, named the full approximation storage (FAS) scheme, to the Kohn–Sham equations for pseudopotential band structure calculations. Traditionally, the nonlinear self-consistent problem is linearized into successive fixed potential eigenvalue problems with potentials updated between them. In the new method, the self-consistent problem is solved directly with the FAS scheme. First, the error of self-consistence in density is calculated; then, an FAS coarse grid problem is defined and solved; finally, a correction is interpolated to the fine grid to modify the density. The eigenvalue problem is integrated inside the FAS scheme, and evolves along with the self-consistent problem within the FAS frame. Calculations are demonstrated for Si and Al.

1. Introduction

Much progress has been made for electron structure calculations of solids within the density functional theory (DFT) [1, 2]. Various methods, such as molecular dynamics, conjugate-gratitude optimization, and the linear scaling method, have been developed for efficient solution of DFT based calculations within the pseudopotential approach [3–9]. Less efficient but more accurate methods have also been developed within the full potential approach [10–13].

In recent years, real space or numerical grid based methods have been extensively investigated [12, 14–22]. One of the motivations to explore the real space method is the availability of advanced numerical algorithms developed in applied mathematics in recent years, such as multigrid algorithms, especially the nonlinear multigrid algorithm [23, 24]. Multigrid algorithms have been found to be especially effective for problems converging slowly with conventional methods.

The Kohn–Sham equations are usually solved by a self-consistent loop in which one repeatedly solves fixed potential eigenvalue problems. The potentials are updated between the eigenvalue problems. The eigenvalue problem is usually expansive to solve, so it is crucial to keep the number of self-consistent iterations minimum in large scale electronic structural calculations. Several methods for the self-consistent problem have been developed, such as the

 © 2005 IOP Publishing Ltd Printed in the UK

DIIS method (direct inversion of iterative subspace) [25, 26], Broyden's method [27, 28], etc. These methods sensitively depend on the initial guess of the potential. If the initial potential is far away from convergence, then these methods may not work or converge slowly.

Brandt has proposed a nonlinear multigrid algorithm, named the full approximation storage (FAS) scheme [23]. The algorithm deals with nonlinear problems as efficiently as linear problems. With this FAS scheme, the entire problem of the nonlinear Kohn–Sham equations may be solved in one shot, without the normal self-consistent loop. Costiner and Ta'asan have tried to solve the Poisson equation and the eigenvalue problem simultaneously [15] with the nonlinear FAS scheme. In realistic density functional theory based electronic structure calculations, in addition to the Hartree potential which may be treated with the Poisson equation, the exchange–correlation potential, which is a functional of the density, also needs be updated simultaneously and self-consistently. This is a problem not treated in the work of Costiner and Ta'asan.

In addition, in pseudopotential based electronic structure calculations, there are both local and nonlocal parts of pseudopotential. Self-consistence is also required in the nonlocal pseudopotentials. In the case of the nonlocal pseudopotentials, Briggs *et al* found that the representation of the nonlocal pseudopotentials on the coarse grid is nontrivial [14]. Ono and Hirose [29] recently proposed a scheme to construct the nonlocal pseudopotentials on the coarse grid. The representation problem may thus be solved.

On the fine grid, one simply calculates the density as the sum of the occupied eigenfunctions. On the coarse grid, the eigenfunctions are neither orthogonal to each other nor normalized even when the original eigenfunctions on the fine grid are exact solutions. If one still defines the density as the sum of the squares of the wavefunctions on the coarse grid as on the fine grid, then it is likely that the total charge is not conserved to the number of electrons. In solid state calculation, if the total charge is not equal to the number of electrons in the periodic unit cell, then the total charge of the system diverges. The representation of the density on the coarse grid is another delicate problem to be treated in the multigrid solution of the Kohn–Sham equations.

In section 2.1, we give a brief introduction of the FAS multigrid algorithm for readers who may not be familiar with this subject. Then in section 2.2, we develop our algorithm by constructing the the nonlinear self-consistent problem based on the density and define the density on the coarse grid. In section 2.3, we discuss the solution of the eigenvalue problem within the FAS framework for density constructed in section 2.2. In section 2.4, we discuss more technical details in constructing various potentials on the coarse grid, including the Hartree potential and exchange–correlation potential, as well as the nonlocal pseudopotential. In section 3, calculations are demonstrated for Si and Al. Section 4 is our conclusion.

2. Method

2.1. The multigrid FAS algorithm

Multigrid algorithms are developed based on observations of numerical experiments for problems such as the Poisson equation,

$$\Delta U = \rho. \tag{1}$$

In the numerical method, the Laplace operator Δ is replaced by simple finite differences. U is the potential to be solved while ρ here is a known charge distribution. Suppose there is an approximate solution, u, such that

$$\Delta u = \rho + d \tag{2}$$

where d is the defect or the residual.

Extensive numerical experiments show that simple relaxation methods, such as the Gauss–Seidel method, are effective in reducing error in the first few iterations, while improvement slows down afterwards. The errors left are mostly of long wavelength in character, and it was found that they could be dumped more effectively on coarse grids. The multigrid idea has thus been discovered and explored.

For the Poisson equation, to get the solution U from the approximation u, one may equally well solve the difference $v = u - U$ which satisfies the following equation:

$$\Delta v = d. \tag{3}$$

A well tested two-level multigrid algorithm for this equation is the following. First, we define a coarse grid problem

$$\Delta^H v^H = d^H \tag{4}$$

where H denotes the coarse grid. d^H is a representation of d on the coarse grid, which can be obtained by averaging or full weighting the function from the fine grid to the coarse grid [30, 31]. The operation is named restriction and is denoted as I_h^H and $d^H = I_h^H d$. Δ^H is the finite difference representation of the Laplace operator on the coarse grid H. An initial approximation for v^H may be obtained from v by restriction, $v_0^H = I_h^H v$. The equation on the coarse grid is then relaxed to improve v^H. The difference $v^H - v_0^H$ is then used to improve the approximate solution on the fine grid by interpolation,

$$v \leftarrow v + I_H^h[v^H - v_0^H]. \tag{5}$$

Here I_H^h is a conventional interpolation operation from the coarse grid to the fine grid, for example linear interpolation.

The operations can be recursively extended to yet coarser grids. By inclusion of multiple levels, errors of all wavelengths may be rapidly damped in the fine grid function. In additional to the effectiveness of the coarse grid in reducing the error of long wavelengths, the coarse grid usually has fewer grid points than the fine grid, so the solution is accelerated with a multigrid algorithm. A multigrid algorithm usually consists of the following steps: (1) initial iterations on the finest level, (2) passage to the sequence of coarser levels where the coarse grid equations are relaxed and (3) return to the finer scale via interpolation correction.

The above scheme applies only to linear problems. For nonlinear problems, it is difficult to define an equation for $v = u - U$. In the FAS method, instead of the difference, $v = u - U$, the desired functions themselves, u, are represented on coarse grids. The equations on a coarser level, however, are modified by an additional term.

$$\Delta^H u^H = \rho^H + \tau^H \tag{6}$$

where

$$\tau^H = \Delta^H I_h^H u - I_h^H \Delta u \tag{7}$$

or

$$\tau^H = \Delta^H I_h^H u - I_h^H \rho - I_h^H d \tag{8}$$

by definition, τ^H are calculated from the quantities available on the fine grid. After the solution u^H is relaxed, the fine grid solution u is updated by

$$u \leftarrow u + I_H^h(u^H - u_0^H) \tag{9}$$

where the initial approximation on the coarse grid is $u_0^H = I_h^H u$. For the Poisson equation with fixed density, one can choose $\rho^H = I_h^H \rho$. A desired principle in the construction of the algorithm is that the coarse grid process should not modify the solution when it is already exact

on the fine grid. For example, if $d = 0$, one reaches $u^H = I_h^H u$ by construction; the correction from the coarse grid is thus zero.

The FAS algorithm has also been applied to differential eigenvalue equations [24], which are nonlinear. The basic steps are similar to that above for the Poisson equation. So a nonlinear problem can be solved as efficiently as a linear problem with FAS.

2.2. *The self-consistent problem*

We proceed to the Kohn–Sham equations [2]

$$[-\tfrac{1}{2}\Delta + v_{\text{eff}}(\mathbf{r}) - \epsilon_i]\psi_i(\mathbf{r}) = 0 \tag{10}$$

$$v_{\text{eff}}(\mathbf{r}) = v_c(\mathbf{r}) + v_{\text{xc}}[\rho(\mathbf{r})] + \sum_i v_{\text{ion}}(\mathbf{r} - \mathbf{R}_i) \tag{11}$$

$$\rho(\mathbf{r}) = \sum_i^{\text{occ}} f_i |\psi_i(\mathbf{r})|^2 \tag{12}$$

where $v_{\text{ion}}(\mathbf{r} - \mathbf{R}_i)$ is the potential due to the ions, and f_i is the occupation number of state i. $v_c(\mathbf{r})$ is the Hartree potential

$$v_c(\mathbf{r}) = \int \frac{\rho(\mathbf{r}')}{|\mathbf{r} - \mathbf{r}'|}\, \mathrm{d}\mathbf{r}', \tag{13}$$

which is equivalent to Poisson's equation:

$$\Delta v_c(\mathbf{r}) = -4\pi\rho(\mathbf{r}). \tag{14}$$

For the exchange–correlation potential $v_{\text{xc}}[\rho(\mathbf{r})]$, the local density approximation [32] has long been the standard choice; more recently the generalized gradient approximations are promoted [33]. In this paper we deal with the exchange–correlation potential in the local density approximation [34]. In order to solve the above equations, one normally starts from a trial input density, $\rho(\mathbf{r})$, then computes the potentials and solves an eigenvalue problem. An output density is then calculated from the eigenfunctions. To construct the self-consistent problem, we use L to represent symbolically the entire process from an initial trial density $\rho(\mathbf{r})$, calculating the potentials and then solving the eigenvalue problem. As a measure of the result of the whole process, the following quantity is calculated at the end:

$$L[\rho(\mathbf{r})] = \sum_i^{\text{occ}} f_i |\psi_i(\mathbf{r})|^2. \tag{15}$$

Self-consistence or convergence then implies

$$L[\rho(\mathbf{r})] = \rho(\mathbf{r}). \tag{16}$$

If there is a defect in self-consistence, then

$$L[\rho(\mathbf{r})] = \rho(\mathbf{r}) + d(\mathbf{r}). \tag{17}$$

According to FAS, one can formally define a coarse grid problem

$$L^H[\rho^H(\mathbf{r})] = \rho^H(\mathbf{r}) + \tau^H(\mathbf{r}) \tag{18}$$

with

$$\tau^H(\mathbf{r}) = L^H[I_h^H \rho(\mathbf{r})] - I_h^H L[\rho(\mathbf{r})]. \tag{19}$$

Compare to the Poisson equation discussed in the above section; the operator Δ is now replaced by L, and Δ^H is replaced by L^H. Here L^H is similar to the operator L but defined on the coarse grid. $L^H[\rho^H(\mathbf{r})]$ implies the whole process from a trial density $\rho^H(\mathbf{r})$, first calculating

the potentials on the coarse grid, and then solving the eigenvalue problem on the coarse grid (to be defined in the next section). As a result, one can define a quantity from the output functions $\psi_i^H(\mathbf{r})$,

$$L^H[\rho^H(\mathbf{r})] = \sum_i^{\text{occ}} f_i |\psi_i^H(\mathbf{r})|^2. \tag{20}$$

The functions $\psi_i^H(\mathbf{r})$ are usually neither orthogonal nor normalized. So the quantity $L^H[\rho^H(\mathbf{r})]$ cannot be regarded simply as the density on the coarse grid. The quantity to be regarded as the density on the coarse grid is $\rho^H(\mathbf{r})$. In principle, it is the self-consistent solution of equation (18). The Hartree potential and exchange–correlation potential on the coarse grid will be calculated from $\rho^H(\mathbf{r})$, instead of from $L^H[\rho^H(\mathbf{r})]$. Our definition of the density is thus different from that of Costiner and Ta'asan.

The above construction provides not only a definition of the density, but also a recursive scheme to update the density on the coarse grid

$$\rho_{j+1}^H(\mathbf{r}) = L^H[\rho_j^H(\mathbf{r})] - \tau^H(\mathbf{r}). \tag{21}$$

Initial density may be chosen as $\rho_0^H(\mathbf{r}) = I_h^H \rho(\mathbf{r})$. On substitution of $\tau^H(\mathbf{r})$, one gets immediately $\rho_1^H(\mathbf{r}) = I_h^H L[\rho(\mathbf{r})]$, where $L[\rho(\mathbf{r})]$ should be available on the fine grid. Self-consistence on the coarse grid can be measured by the norm of the difference $\rho_j^H(\mathbf{r}) - \rho_{j+1}^H(\mathbf{r})$.

Once self-consistence converges on the coarse grid, correction is made to the fine grid solution by

$$\rho(\mathbf{r}) \leftarrow \rho(\mathbf{r}) + I_H^h[\rho^H(\mathbf{r}) - \rho_0^H(\mathbf{r})]. \tag{22}$$

If the solution on the fine grid is already self-consistent, i.e. $d(\mathbf{r}) = 0$, the recursive procedure leads to $\rho^H(\mathbf{r}) = I_h^H \rho(\mathbf{r})$, so the correction to the original solution $\rho(\mathbf{r})$ is zero. The algorithm is thus stationary at the exact solution, as desired.

Self-consistency on the fine grid implies $\rho^H(\mathbf{r}) = I_h^H \rho(\mathbf{r})$ on the coarse grid, instead of $\rho^H(\mathbf{r}) = L^H[\rho^H(\mathbf{r})]$ as one might mistakenly infer from the fine grid. This definition thus insures that the total density on the coarse grid is conserved; both the Poisson equation and the exchange–correlation potential will thus behave properly. Costiner and Ta'asan [15] defined $L^H[\rho^H(\mathbf{r})]$ as the density on the coarse grid. For the stable solution of the Poisson equation, an additional global constant is imposed. Since they did not consider the exchange–correlation potential, the side effect of their density on the exchange–correlation potential did not show up in their test case.

Now let us compare the above algorithm with the traditional simple mixing scheme to update a new trial density from a previous iteration,

$$\rho(\mathbf{r}) \leftarrow \rho(\mathbf{r}) + \alpha d(\mathbf{r}). \tag{23}$$

The mixing parameter, α, is typically chosen in the range [0, 1]. In plane wave calculations, it has been observed that for plane waves of long wavelengths, α should be chosen smaller than that for the part of short wavelengths [35]. A smaller α means the input density changes little, which may stabilize the iteration but slows down the convergence. The long wavelength part is thus the difficult part in a self-consistent problem. The long wavelength part is better represented on the coarse grid than on the fine grid. If we compare equation (23) with (22), we see the difference in the correction term. In equation (23), the correction is a simple scaling of the defect. The scaling parameter may be optimized by the DIIS technique [25]. There is no guarantee that defects on different grid points deviate in the same direction and can be adjusted by a single parameter. Equation (22) is obviously more powerful since it deals with each coarse grid point individually.

2.3. The eigenvalue problem

The operators L and L^H consists of two major operations; one is the calculation of the potentials and another is the eigenvalue problem. In this section we deal with the eigenvalue problem.

Suppose we have a set of approximate eigenfunctions $\psi_i(\mathbf{r})$; their defects are

$$d_i(\mathbf{r}) = [-\tfrac{1}{2}\Delta + v_{\text{eff}}(\mathbf{r}) - \epsilon_i]\psi_i(\mathbf{r}). \tag{24}$$

Following the FAS scheme outlined in section 2.1, we can construct the coarse grid problem as

$$[-\tfrac{1}{2}\Delta^H + v^H_{\text{eff}}(\mathbf{r}) - \epsilon_i]\psi^H_i(\mathbf{r}) = \tau^H_i(\mathbf{r}), \tag{25}$$

with

$$\tau^H_i(\mathbf{r}) = [-\tfrac{1}{2}\Delta^H + v^H_{\text{eff}}(\mathbf{r}) - \epsilon_i]\bar{I}^H_h\psi_i(\mathbf{r}) - I^H_h d_i(\mathbf{r}). \tag{26}$$

In the FAS scheme [24], one may define a different restriction operator, $\bar{I}^H_h$, on the eigenfunction ψ_i, from the restriction operator, I^H_h, on the defect. To simplify the calculation, we require that $\bar{I}^H_h\psi_i(\mathbf{r})$ be normalized. This can be done by simple scaling after normal restriction operation. A normalized eigenfunction on the coarse grid implies an equal contribution to one electron charge in the measure $L^H[\rho^H(\mathbf{r})]$. In the scheme developed by Brandt *et al* for the fixed potential differential eigenvalue problem, normalization is not necessary as long as one tracks the norm of each eigenfunction before restriction, and restores it afterward [24]. With normalization, the tracking of the norm for each eigenfunction is simplified, while its side effect on the solution of the eigenvalue problem is negligible.

With substitution of τ^H, equation (25) can also be written as

$$[-\tfrac{1}{2}\Delta^H + v^H_{\text{eff}}(\mathbf{r}) - \epsilon_i][\psi^H_i(\mathbf{r}) - \bar{I}^H_h\psi_i(\mathbf{r})] = -I^H_h d_i(\mathbf{r}). \tag{27}$$

The coarse grid equation thus seeks a solution of the difference $\psi^H_i(\mathbf{r}) - \bar{I}^H_h\psi_i(\mathbf{r})$ corresponding to a defect $I^H_h d_i(\mathbf{r})$ but with opposite sign. To reduce the defect in the equation (24), the new solution on the fine grid should be constructed as

$$\psi_i(\mathbf{r}) \leftarrow \psi_i(\mathbf{r}) + I^h_H[\psi^H_i(\mathbf{r}) - \bar{I}^H_h\psi_i(\mathbf{r})]. \tag{28}$$

At convergence, i.e. $d_i(\mathbf{r}) = 0$, with an iterative relaxation procedure, one has $\psi^H_i(\mathbf{r}) = \bar{I}^H_h\psi_i(\mathbf{r})$. So the exact solution is stationary by construction.

The potentials $v^H_{\text{eff}}(\mathbf{r})$ are to be defined. Any nonsingular potential defined on the coarse grid is legitimate at the exact solution. This is guaranteed by the construction. However, when the solution is approximate, the better one defines the potential on the coarse grid the faster the solution converges. For a fixed potential problem, one may define the potential on the coarse grid as the restriction from that on the fine grid [13, 24]. For a self-consistent problem, it is natural to calculate a potential directly according to the density available on the coarse grid. So the eigenfunction can be relaxed with potentials already updated on the coarse grid. Self-consistence is thus accelerated within the FAS solution process for the eigenvalue problem.

Self-consistence on the coarse grid converges much faster than that on the fine grid due to the specific form of the coarse grid equations. The error in the potential affects the difference $\psi^H_i(\mathbf{r}) - \bar{I}^H_h\psi_i(\mathbf{r})$ rather than $\psi^H_i(\mathbf{r})$ itself. They may differ by orders of magnitude after a reasonable initialization. This will significantly reduce error in the eigenfunctions $\psi^H_i(\mathbf{r})$, which may lead to charge sloshing. Our test calculations show that one or two updates of potentials are sufficient to raise self-consistence significantly on the coarse grid.

For relaxation, we use the Gauss–Seidel method. For the Kohn–Sham eigenvalue equations, it implies the following update:

$$\psi_i(\mathbf{r}) \leftarrow \psi_i(\mathbf{r}) - \frac{d_i(\mathbf{r})}{\text{diag} + v_{\text{eff}}(\mathbf{r}) - \epsilon_i} \tag{29}$$

on the fine grid, and

$$\psi_i^H(\mathbf{r}) \leftarrow \psi_i^H(\mathbf{r}) - \frac{d_i^H(\mathbf{r})}{\mathrm{diag}^H + v_{\mathrm{eff}}^H(\mathbf{r}) - \epsilon_i} \tag{30}$$

on the coarse grid with $d_i^H(\mathbf{r}) = [-\frac{1}{2}\Delta^H + v_{\mathrm{eff}}^H(\mathbf{r}) - \epsilon_i]\psi_i^H(\mathbf{r}) - \tau_i^H(\mathbf{r})$. diag and diag^H come from the diagonal part of the kinetic operator. For example, the kinetic operator is $-\frac{1}{2}\Delta$ on the fine grid. If one uses $\frac{\mathrm{d}^2}{\mathrm{d}x^2} f(i) = 1/(h^2)[f(i-1) + f(i+1) - 2f(i)]$ in each direction of the axes, then diag $= 3/h^2$ in 3d.

After the Gauss–Seidel step, the defect at point i becomes zero. This is the ideal solution. However, a new defect may come up when the next grid point, for example $i+1$, is updated. So the grid usually needs to be swept a few times (three in the test) to smooth down the error sufficiently. One can also use other methods for relaxation, such as the Jacobi method [31], the Kaczmarz method [37], DIIS [25, 26], and conjugate gradient optimization. The Gauss–Seidel method is both simple enough and efficient.

To prevent the eigenfunctions from collapsing onto each other, the Gram–Schmidt orthogonal procedure follows.

$$\psi_i \leftarrow \psi_i - \sum_{j<i} \frac{\langle \psi_j, \psi_i \rangle}{\langle \psi_j, \psi_j \rangle} \psi_j. \tag{31}$$

The Gram–Schmidt procedure is a sequential method; it can be implemented immediately after each eigenfunction being relaxed. The later eigenfunction is always orthogonalized to newly updated eigenfunctions. The orthogonal condition on the coarse grid is imposed on the difference $\psi_i^H - \bar{I}_h^H \psi_i$ rather than ψ_i^H itself,

$$\psi_i^H \leftarrow \psi_i^H - \sum_{j<i} \frac{\langle \psi_j^H, \psi_i^H - \bar{I}_h^H \psi_i \rangle}{\langle \psi_j^H, \psi_j^H \rangle} \psi_j^H. \tag{32}$$

This condition ensures that the solution will be stationary when it is exact. Normalization is immediately applied after orthogonalization for each eigenfunction, which has the effect to suppresses possible divergence due to relaxation [19]. The denominators in the above equations may be replaced by $\langle \psi_j, \psi_j \rangle = 1$ and $\langle \psi_j^H, \psi_j^H \rangle = 1$, because when one updates the eigenfunction ψ_i, ψ_j with $j < i$ has already been normalized.

The eigenvalues are updated by the Rayleigh quotient method, which globally minimizes the residues in the least-squares sense [36]. In order to avoid round-off error in processing small numbers, the following formula is used:

$$\epsilon_i \leftarrow \epsilon_i + \frac{\langle \zeta_i, \eta_i \rangle}{\langle \zeta_i, \zeta_i \rangle} \tag{33}$$

where

$$\begin{aligned} \zeta_i &= \psi_i^H(\mathbf{r}) + I_h^H \psi_i(\mathbf{r}) - \bar{I}_h^H \psi_i(\mathbf{r}) \\ \eta_i &= [-\tfrac{1}{2}\Delta^H + v_{\mathrm{eff}}^H(\mathbf{r}) - \epsilon_i]\psi_i^H(\mathbf{r}) - \tau_i^H(\mathbf{r}) \end{aligned} \tag{34}$$

on the coarse grid, and $\zeta_i = \psi_i(\mathbf{r})$, $\eta_i = d_i(\mathbf{r})$ on the fine grid.

Relaxation, orthonormalization and Rayleigh quotient calculation are the basic operations in our algorithm for the eigenvalue problem. One can solve the eigenvalue problem based on these operations alone by iterations on the fine grid. However, the multigrid algorithm considerably speeds up the solution.

Our algorithm for the eigenvalue problem is based on the ideas developed by Brandt *et al* [24]. Costiner and Ta'asan [15] developed their own method for the eigenvalue problem. They apply FAS in the Rayleigh–Ritz subspace of the eigenvalue problem, resulting in a generalized

eigenvalue problem on the coarse grid. Since there are mixing and permutation of eigenvectors during matrix diagonalization on the coarse grid, tracking of eigenvectors between the fine grid and the coarse grid becomes complicated. Our algorithm is simpler than their method in tracking the eigenfunctions between the coarse grid and fine grid. As found in the paper [24], it is enough to implement the Rayleigh–Ritz procedure or subspace rotation [7] on the fine grid after the FAS procedure.

2.4. The potentials

In this section, we discuss the calculation of the various parts of the potential in realistic calculations.

In the numerical method, the Hartree potential is calculated more efficiently by the Poisson equation than computing the integral of equation (13). For the integral one needs to sum over all grid points, while in the Poisson equation using a differential operator one only needs a few local grid points to update the potential at each grid point.

Since the density changes on the coarse grid, we use the FAS scheme (see section 2.1) to solve the Poisson equation. In the normal Poisson equation with the density fixed, one takes $\rho^H = I_h^H \rho$. In the self-consistent problem, the density on the coarse grid is taken from $\rho^H(\mathbf{r}) = L^H[\rho^H(\mathbf{r})] - \tau^H(\mathbf{r})$. We use the Gauss–Seidel method for the relaxation of the Poisson equation.

For the solution process to be stable, it is desirable that the total charge entering the Poisson equation be zero. This is realized along with the calculation of ionic potential with the Ewald technique [38]. In this technique, a negative charge distribution, usually a Gaussian distribution,

$$\rho_i(r) = \frac{Z}{\sqrt{\pi^3} r_c^3} \mathrm{e}^{-(r/r_c)^2} \tag{35}$$

is added to each ion. The potential from each Gaussian density has the form of an error function divided by r [39].

$$v_i(r) = \frac{Z \operatorname{erf}(r/r_c)}{r}. \tag{36}$$

This potential has an asymptotic tail that compensates the long range Coulomb tails from the ion. The screened ionic potential is then short ranged. The calculation of the crystal ionic potential thus extends only up to the atoms in the neighbouring cells.

To compensate the artificial Gaussian charges added to the ions, the total charge of opposite sign from the Gaussian distributions is added to the electronic charge. The total charge from both the Gaussian charges and the electronic charge in the Poisson equation is then zero. The Poisson equation to be solved is $\Delta V_c(\mathbf{r}) = -4\pi\rho_{\mathrm{tot}}(\mathbf{r})$, with $\rho_{\mathrm{tot}}(\mathbf{r}) = \rho(\mathbf{r}) - \sum_i \rho_i$.

The choice of Gaussian screening parameter, r_c, is quite empirical. Since we use Kleinman–Bylander type separable pseudopotentials [40, 41], $v_{\mathrm{ion}}(\mathbf{r} - \mathbf{R}_i) = V_{\mathrm{L}} + V_{\mathrm{NL}}$, where V_{L} is the long ranged local part of the pseudopotential and V_{NL} is the short ranged nonlocal part of the pseudopotential. We fix r_c such that the screened local potential, $V_{\mathrm{L}} + v_i$, is zero at the nuclei. The value of v_i at the nuclei is $\frac{2Z}{\sqrt{\pi} r_c}$. The result for Si is shown in figure 1. The advantage of this choice is that the screened potential, $V_{\mathrm{L}} + v_i$, is zero at both origin and distance, so it becomes much smoother than other methods, such as that in the SIESTA code [9]. The smoothness of the potential improves the accuracy of the representation on the coarse grid by restriction.

To represent the nonlocal pseudopotential on a grid, filtering techniques have been developed to remove the high frequency components in the pseudopotentials [14, 42].

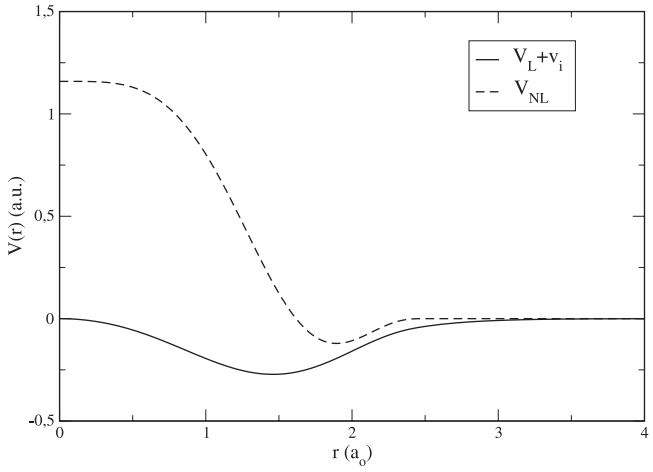

Figure 1. Ionic potentials for Si. The solid line shows the screened local potential and the broken line shows the nonlocal pseudopotential ($l = 0$ is the local part).

Ono and Hirose [29] recently proposed a double-grid scheme to obtain accurate nonlocal pseudopotentials on a grid. The nonlocal pseudopotential projector on a given grid is restricted by full weighting from that prepared on a much finer grid. For example, for the pseudopotential projector on a grid h, one may prepare the projector on a finer grid with spacing $h/2$, and then restrict it to the grid h. The projector on a coarse grid of spacing $H = 2h$ can be restricted from the projector on the grid h. The nonlocal pseudopotential operator on the coarse grid is

$$V_{\mathrm{NL}}^{H}(\mathbf{r}) = \sum_{lm} \frac{|(\Delta V_l \phi_{lm})^H\rangle\langle(\Delta V_l \phi_{lm})^H|}{\langle\phi_{lm}|\Delta V_l|\phi_{lm}\rangle}. \tag{37}$$

Since the projectors $\Delta V_l \phi_{lm}$, $(\Delta V_l \phi_{lm})^H$ are short ranged in space, we need only take into account those grid points that are within a cut-off radius around each ion.

In solid state calculations, the eigenfunctions take the Bloch form $\psi_{\mathbf{k}}(\mathbf{r}) = \mathrm{e}^{(-\mathrm{i}\mathbf{k}\cdot\mathbf{r})} u_{\mathbf{k}}(\mathbf{r})$ where $u_{\mathbf{k}}(\mathbf{r})$ is periodic. The operation of the nonlocal pseudopotential operator $V_{\mathrm{NL}}^{H}(\mathbf{r})$ on $\psi_{\mathbf{k}}(\mathbf{r})$ can be reduced as

$$\begin{aligned} V_{\mathrm{NL}}\psi_{\mathbf{k}}(\mathbf{r}) &= \sum_{lm} \frac{|\Delta V_l \phi_{lm}\rangle\langle\Delta V_l \phi_{lm}|\mathrm{e}^{-\mathrm{i}\mathbf{k}\cdot\mathbf{r}} u_{\mathbf{k}}(\mathbf{r})\rangle}{\langle\phi_{lm}|\Delta V_l|\phi_{lm}\rangle} \\ &= \sum_{lm} \frac{|\Delta V_l \phi_{lm}\rangle\langle\Delta V_l \phi_{lm}\mathrm{e}^{\mathrm{i}\mathbf{k}\cdot\mathbf{r}}|u_{\mathbf{k}}(\mathbf{r})\rangle}{\langle\phi_{lm}|\Delta V_l|\phi_{lm}\rangle} \\ &= \sum_{lm} \frac{|\Delta V_l \phi_{lm}\mathrm{e}^{\mathrm{i}\mathbf{k}\cdot\mathbf{r}}\rangle\langle\Delta V_l \phi_{lm}\mathrm{e}^{\mathrm{i}\mathbf{k}\cdot\mathbf{r}}|u_{\mathbf{k}}(\mathbf{r})\rangle}{\langle\phi_{lm}|\Delta V_l|\phi_{lm}\rangle}\mathrm{e}^{-\mathrm{i}\mathbf{k}\cdot\mathbf{r}} \\ &= [V'_{\mathrm{NL}} u_{\mathbf{k}}(\mathbf{r})]\mathrm{e}^{-\mathrm{i}\mathbf{k}\cdot\mathbf{r}}. \end{aligned} \tag{38}$$

The equations to be solved for $u_{\mathbf{k}}(\mathbf{r})$ then take the form

$$[-\tfrac{1}{2}\Delta + \mathrm{i}\mathbf{k}\cdot\nabla + \tfrac{1}{2}|\mathbf{k}|^2 + V_{\mathrm{eff}}(\mathbf{r}) - \epsilon_{\mathbf{k}}]u_{\mathbf{k}}(\mathbf{r}) = 0 \tag{39}$$

with $V_{\mathrm{eff}}(\mathbf{r}) = v_{\mathrm{xc}}[\rho(\mathbf{r})] + V_c(\mathbf{r}) + V_{c\mathrm{Loc}}(\mathbf{r}) + V'_{\mathrm{NL}}(\mathbf{r})$, where $V_{c\mathrm{Loc}}$ is the sum of local potentials $V_{\mathrm{L}} + v_i$ from atoms up to the neighbouring cells. $V_c(\mathbf{r})$ comes from solving the Poisson equation $\Delta V_c(\mathbf{r}) = -4\pi\rho_{\mathrm{tot}}(\mathbf{r})$. The band index at each $\mathbf{k}$ point is implied here.

The equation on the coarse grid can be written down similarly to equation (25).

$$[-\tfrac{1}{2}\Delta^H + \mathrm{i}\mathbf{k}\cdot\nabla^H + \tfrac{1}{2}|\mathbf{k}|^2 + V_{\mathrm{eff}}^H(\mathbf{r}) - \epsilon_{\mathbf{k}}]u_{\mathbf{k}}^H(\mathbf{r}) = \tau_{\mathbf{k}}^H(\mathbf{r}) \tag{40}$$

with

$$\tau_{\mathbf{k}}^H(\mathbf{r}) = [-\tfrac{1}{2}\Delta^H + \mathrm{i}\mathbf{k}\cdot\nabla^H + \tfrac{1}{2}|\mathbf{k}|^2 + V_{\mathrm{eff}}^H(\mathbf{r}) - \epsilon_{\mathbf{k}}]\bar{I}_h^H u_{\mathbf{k}}(\mathbf{r}) - I_h^H d_{\mathbf{k}}(\mathbf{r}) \tag{41}$$

where $d_{\mathbf{k}}(\mathbf{r})$ is the defect on the fine grid. $V_{\mathrm{eff}}^H(\mathbf{r}) = v_{\mathrm{xc}}^H[\rho^H(\mathbf{r})] + V_c^H(\mathbf{r}) + V_{c\mathrm{Loc}}^H(\mathbf{r}) + V_{\mathrm{NL}}'^H(\mathbf{r})$. $v_{\mathrm{xc}}^H[\rho^H(\mathbf{r})]$ can be calculated directly from the density $\rho^H(\mathbf{r})$. $V_c^H(\mathbf{r})$ comes from the Poisson equation. $V_{c\mathrm{Loc}}^H(\mathbf{r})$ is the restriction of $V_{c\mathrm{Loc}}(\mathbf{r})$. $V_{\mathrm{NL}}'^H(\mathbf{r})$ is similar to $V_{\mathrm{NL}}'(\mathbf{r})$ except the replacement of $(\Delta V_l\phi_{lm})^H$ for $\Delta V_l\phi_{lm}$.

For the calculation of the nonlocal pseudopotential, one needs to first prepare the integral $\langle\Delta V_l\phi_{lm}\mathrm{e}^{\mathrm{i}\mathbf{k}\cdot\mathbf{r}}|u_{\mathbf{k}}(\mathbf{r})\rangle$. This integral is treated as a constant during relaxation. Relaxation is followed by orthogonalization and normalization. The nonlocal pseudopotentials are updated after the normalization, as is the eigenvalue. Since one would repeat relaxation of the Kohn–Sham equations a few times, the nonlocal pseudopotential is updated during this cycle to improve self-consistence.

3. Calculations

We have elaborated enough detail for the solution of the Kohn–Sham equations. We now outline the major steps with the multigrid method proposed above.

There can be different ways to prepare the initial approximation. Here for the initial density we choose a uniform constant distribution normalized to the number of electrons. The potentials are then calculated on the fine grid and the total potential is restricted to the coarse grid. Each eigenfunction is first initialized with random numbers on the coarse grid and relaxed. The eigenfunctions are then interpolated to the fine grid and normalized. A new density on the fine grid is then calculated and potentials are updated. Each eigenfunction is then sequentially improved by a fixed potential FAS algorithm, with a Ritz procedure at the end. The procedures are well described in the paper for the fixed potential eigenvalue problem [24].

From here we begin the self-consistent FAS cycle presented in the present paper. We follow a general paradigm of the multigrid method, a two-level V-cycle, i.e. from the fine grid to the coarse grid and then from the coarse grid to the fine grid.

(1) On the fine grid, we calculate the density from the eigenfunction and then potentials, then solve the eigenvalue problem. Those procedures are repeated three times to smooth the short wavelength error in self-consistence on the fine grid.
(2) Next, we apply the fixed potential eigenvalue algorithm [24], so that defects in self-consistence can be estimated. Convergence is checked here to see whether further calculation should be considered.
(3) If the convergence is not reached, we restrict the density to coarse grid and calculate the potentials there. Then eigenfunctions are restricted from the fine grid and relaxed one after another, while each later eigenfunction is orthogonalized to all the newly updated eigenfunctions by the Gram–Schmidt procedure. After all the eigenvectors finish, the density is calculated again and self-consistence is checked to decide whether or not to proceed with another iteration on the coarse grid.
(4) On returning to the fine grid, we interpolate the correction in density from the coarse grid to the fine grid, then update the potentials on the fine grid. The eigenfunctions on the fine grid are then interpolated and followed by a relaxation and Gram–Schmidt procedure. We then go back to step (1).

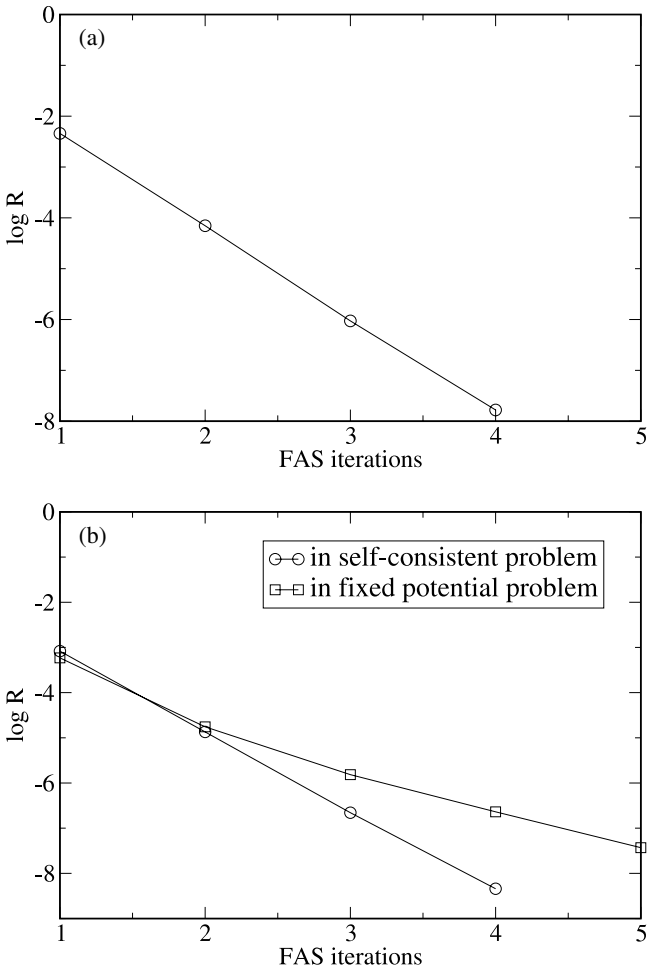

Figure 2. Convergence of (a) density and (b) eigenvalues with respect to the number of FAS V-cycles. For the self-consistent eigenvalue problem, the density and the eigenfunctions converge simultaneously.

Figure 2 shows the convergence behaviour for Si. The calculation is done with a cubic cell of eight Si atoms with a lattice constant 5.38 Å. The fine grid has $16 \times 16 \times 16$ points. The convergence is based on the norm of the residues. The convergence in eigenvalues is represented by the lowest eigenfunction, the behaviour of other eigenfunctions is slightly different due to additional orthogonal constraints. For the self-consistent problem, the density and the eigenvalues converge simultaneously in this algorithm. The potential used in the fixed potential case is based on a uniform charge density. Since the algorithm is iterative in nature, it is normal to have a few FAS iterations even for the fixed potential problem. We see that the self-consistent problem may not be necessarily harder to converge than a fixed potential eigenvalue problem with FAS.

To calculate the density of states (DOS), a set of 56 special k-points is generated with the Monkhorst–Pack scheme [43] from a mesh of $10 \times 10 \times 10$ in the Brillouin zone. The DOS calculated with the smearing method of Methfessel and Paxton [44] ($W = 0.6$ eV and $N = 2$) is shown in figure 3, along with that calculated from a plane wave code using the

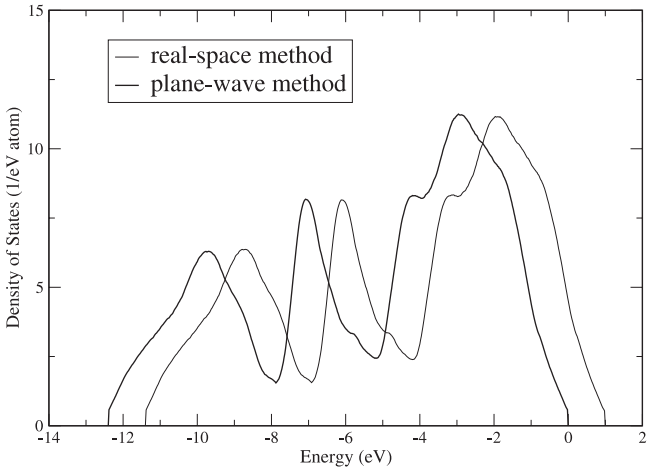

Figure 3. Density of states for Si.

Table 1. Convergence behaviour in the sequential-update method.

Iteration	Residual in self-consistence
1	$3.602\,006 \times 10^{-4}$
2	$3.184\,831 \times 10^{-5}$
3	$4.141\,065 \times 10^{-5}$
4	$5.706\,036 \times 10^{-5}$
5	$7.890\,775 \times 10^{-5}$
6	$1.092\,712 \times 10^{-4}$

same pseudopotentials with a cut-off energy $E_{\text{cut}} = 5$ au. The DOS from the real space method agrees well with that of plane wave calculations up to a shift in energy. In plane wave calculations, the eigenvalues are shifted by the $G = 0$ term [45]. In the real space method, the eigenvalues are solved up to a constant by the differential Poisson equation under periodic conditions. The calculation with many k-points converges slightly faster than that with a single Γ-point.

For calculation of a semiconductor or an insulator, the occupation number $f_{n,\mathbf{k}}$ can be fixed in advance. In the case of a metal, there may be several bands with very close or degenerate energies at the Fermi level. If occupation switches from one eigenfunction to another at the Fermi level, the density will fluctuate dramatically. In this case, we sample the occupation according to a Fermi distribution with a finite temperature. The occupation numbers are treated as constant throughout the FAS cycle and updated only at the begin of the FAS cycle. For fcc Al with a lattice constant 7.525 a_0, we can get convergence in self-consistence in density $1.347\,534 \times 10^{-3}$ after initialization, and $3.373\,354 \times 10^{-4}$ after the first three self-consistent iterations on the fine grid. From here we make two calculations to compare the sequential-update method and the present nonlinear method. In the sequential-update method, the eigenvalue problem and the update of the potentials are repeated sequentially. The eigenvalue problem is solved with the fixed potential algorithm [24]. The result is shown in table 1. We see that the simple sequential-update method converges slowly and fluctuates. However, with the nonlinear procedure to update the density, self-consistence reaches $3.471\,7692 \times 10^{-6}$ in one FAS cycle, demonstrating the effectiveness of the algorithm.

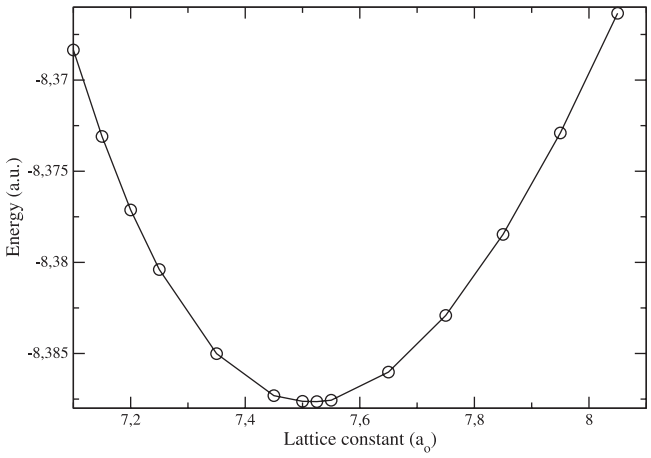

Figure 4. Total energy versus lattice constant for Al.

Total energy is an important quantity from a DFT calculation. In this algorithm, the total energy need only be calculated once at convergence. Using the Laplace transform, $\frac{1}{r} = \pi^{\frac{1}{2}} \int_0^\infty \mathrm{e}^{-sr^2} s^{\frac{1}{2}}\,\mathrm{d}s$ and the product property of two Gaussian functions, one can derive the formula for the total energy

$$\begin{aligned} E = \sum_{n,\mathbf{k}} f_{n,\mathbf{k}} \langle u_{n,\mathbf{k}} | -\tfrac{1}{2}\Delta + \mathrm{i}\mathbf{k}\cdot\nabla + \tfrac{1}{2}|\mathbf{k}|^2 | u_{n,\mathbf{k}} \rangle \\ + \sum_{n,\mathbf{k},lm} f_{n,\mathbf{k}} \frac{|\langle u_{n,\mathbf{k}}(\mathbf{r}) | \Delta V_l \phi_{lm} \mathrm{e}^{\mathrm{i}\mathbf{k}\cdot\mathbf{r}} \rangle|^2}{\langle \phi_{lm} | \Delta V_l | \phi_{lm} \rangle} + E_{\mathrm{xc}}[\rho(\mathbf{r})] \\ + \tfrac{1}{2} \int \mathrm{d}\mathbf{r}\, \rho_{\mathrm{tot}}(\mathbf{r}) V_c(\mathbf{r}) + \int \mathrm{d}\mathbf{r}\, V_{c\mathrm{Loc}}(\mathbf{r}) \rho(\mathbf{r}) \\ + \frac{1}{2} \sum_{i \neq j} \frac{Z_i Z_j}{R_{ij}} \mathrm{erfc}\left(\frac{R_{ij}}{\sqrt{r_{c,i}^2 + r_{c,j}^2}} \right) - \frac{1}{\sqrt{2\pi}} \sum_i \frac{Z_i^2}{r_{c,i}}. \end{aligned} \tag{42}$$

Here $f_{n,\mathbf{k}}$ is the occupation number for the band n and the $\mathbf{k}$ point. The index lm is the angular moment. Summation over all atoms in the unit cell is implied in the calculation of the nonlocal potential energy, even though the potential from the Poisson equation is solved up to a constant under periodic boundary conditions. The total energy, however, is not affected by the constant because the total charge from $\rho_{\mathrm{tot}}(\mathbf{r})$ is zero. R_{ij} is the distance between ion i and j. Z_i is the ion charge and $r_{c,i}$ is the parameter of the Gaussian screening charge for atom i. In $\sum_{i \neq j}$, the index i is taken in the unit cell and j up to the neighbouring cells. The index i in the last term runs over atoms in the unit cell.

The variation of total energy with the lattice constant for Al is displayed in figure 4. The calculations are based on a real space mesh of $16 \times 16 \times 16$ and a set of 56 special k-points. The total energy reaches a minimum -8.3876 au (-2.0969 au/atom) at the lattice constant 7.525 a_0. The atomic total energy is -1.946 au, which results in a cohesive energy of 4.1 eV/atom. The experimental result is 3.32 eV/atom and the theoretical result with the muffin-tin approximation is 3.84 eV/atom [46].

4. Conclusion

The self-consistent problem is usually linearized into successive eigenvalue problems with a potential update in between. In the present paper, a nonlinear FAS algorithm is framed for the self-consistent problem. First, the error of self-consistence in density is calculated, and then an FAS coarse grid problem is defined and solved; finally, a correction is interpolated to the fine grid to modify the density. The eigenvalue problem and update of the potentials are integrated into the same FAS frame. Within this FAS frame, the eigenvalue problem evolves simultaneously along with the self-consistent problem. For example, as FAS returns to the fine grid, the eigenvalue problem will be improved with the density already updated.

The nonlinear FAS algorithm for the self-consistent problem avoids some problems intrinsic to the sequential-update method, such as fluctuation. The ideas developed in this paper may suggest a new way to solve the self-consistent problem in many other areas.

Acknowledgments

The author Jian Wang would like to thank Professors A Brandt, T L Beck, H Eschrig, M Parrinello, and J L Martins for much help during this work.

References

[1] Hohenberg P and Kohn W 1964 *Phys. Rev.* **136** B864
[2] Kohn W and Sham L J 1965 *Phys. Rev.* **140** A1133
[3] Car R and Parrinello M 1985 *Phys. Rev. Lett.* **55** 2471
[4] Payne M C, Teter M P, Allan D C, Arias T A and Joannopoulos J D 1992 *Rev. Mod. Phys.* **64** 1045
[5] Kim J, Mauri F and Galli G 1995 *Phys. Rev.* B **52** 1640
[6] Martins J L and Cohen M L 1988 *Phys. Rev.* B **37** 6134
[7] Kresse G and Furthmüller J 1996 *Phys. Rev.* B **54** 11169
Kresse G and Furthmüller J 1996 *Comput. Mater. Sci.* **6** 15
[8] Bowler D R and Gillan M J 1998 *Comput. Phys. Commun.* **112** 103
[9] Soler J M, Artacho E, Gale J D, Garcia A, Junquera J, Ordejon P and Sanchez-Portal D 2002 *J. Phys.: Condens. Matter* **14** 2745
[10] Blaha P, Schwarz K, Madsen G, Kvasnicka D and Luitz J 1999 *WIEN2k, An Augmented Plane Wave + Local Orbitals Program for Calculating Crystal Properties* ed K Schwarz (Technical Universitat Wien, Austria) ISBN 3-9501031-1-2
[11] Koepernik K and Eschrig H 1999 *Phys. Rev.* B **59** 1743
[12] Beck T L 2000 *Rev. Mod. Phys.* **72** 1041
[13] Wang J and Beck T L 2000 *J. Chem. Phys.* **112** 9223
Wang J and Stuchebrukhov A A 2000 *Int. J. Quantum Chem.* **80** 591
[14] Briggs E L, Sullivan D J and Bernholc J 1996 *Phys. Rev.* B **54** 14362
[15] Costiner S and Ta'asan S 1995 *Phys. Rev.* E **51** 3704
Costiner S and Ta'asan S 1995 *Phys. Rev.* E **52** 1181
[16] Modine N A, Zumbach G and Kaxiras E 1997 *Phys. Rev.* B **55** 10289
[17] Gygi F and Galli G 1995 *Phys. Rev.* B **52** R2229
[18] Chelikowsky J R, Troullier N and Saad Y 1994 *Phys. Rev. Lett.* **72** 1240
[19] Grinstein F F, Rabitz H and Askar A 1983 *J. Comput. Phys.* **51** 423
[20] Heiskanen M, Torsti T, Puska M J and Nieminen R M 2001 *Phys. Rev.* B **63** 245106
[21] Kopylow A V, Heinemann D and Kolb D 1998 *J. Phys. B: At. Mol. Opt. Phys.* **31** 4743
[22] Lee I H, Kim Y H and Martin R M 2000 *Phys. Rev.* B **61** 4397
[23] Brandt A 1977 *Math. Comput.* **31** 333
[24] Brandt A, McCormick S and Ruge J 1983 *SIAM J. Sci. Stat. Comput.* **4** 244
[25] Pulay P 1980 *Chem. Phys. Lett.* **73** 393
[26] Wood D M and Zunger A 1985 *J. Phys. A: Math. Gen.* **18** 1343
[27] Vanderbilt D and Louie S G 1984 *Phys. Rev.* B **30** 6118

[28] Johnson D D 1988 *Phys. Rev.* B **38** 12807
[29] Ono T and Hirose K 1999 *Phys. Rev. Lett.* **82** 5016
[30] Hackbusch W (ed) 1985 *Multigrid Methods and Applications* (Berlin: Springer)
[31] Press W H, Teukolsky S A, Vetterling W T and Flannery B P 1996 *Numerical Recipes in C* (Cambridge: Cambridge University Press)
[32] Jones R O and Gunnarsson O 1989 *Rev. Mod. Phys.* **61** 689
[33] Kohn W, Becke A D and Parr R G 1996 *J. Chem. Phys.* **100** 12974
[34] Perdew J P and Zunger A 1981 *Phys. Rev.* B **23** 5048
[35] Kerker G P 1981 *Phys. Rev.* B **23** 3082
[36] Axelsson O 1996 *Iterative Solution Method* (Cambridge: Cambridge University Press)
[37] Tanabe K 1971 *Numer. Math.* **17** 203
[38] Allen M P and Tildesley D J 1990 *Computer Simulation of Liquids* (Oxford: Oxford Science Publications) p 156
[39] Eschrig H 1989 *Optimized LCAO Method* (Berlin: Springer) p 133
[40] Kleinman L and Bylander D M 1982 *Phys. Rev. Lett.* **48** 1425
[41] Troullier N and Martins J L 1991 *Phys. Rev.* B **43** 1993
[42] King-Smith R D, Payne M C and Lin J S 1991 *Phys. Rev.* B **44** 13063
[43] Monkhorst H J and Pack J D 1976 *Phys. Rev.* B **13** 5188
[44] Methfessel M and Paxton A T 1989 *Phys. Rev.* B **40** 3616
[45] Ihm J, Zunger A and Cohen M L 1979 *J. Phys. C: Solid State Phys.* **12** 4409
[46] Janak J F, Moruzzi V L and Williams A R 1975 *Phys. Rev.* B **12** 1257